Pullout forces and friction in multiwall carbon nanotubes

Z. Xia and W. A. Curtin
Division of Engineering, Brown University, Providence, Rhode Island 02912 USA
(Received 7 April 2004; published 30 June 2004)

Molecular dynamic calculations of pullout in multiwall carbon nanotubes (CNTs) demonstrate that inner walls with fractured ends have pullout forces $\sim 3-4$ times larger than those for capped ends, due to deformation of the fractured end, quantitatively accounting for experiments. Under pressure, Amonton's law applies to an area of contact at the fractured end, with $\mu = 0.13-0.33$. Defects in the CNT walls affect the force, suggesting a mechanism for the observed stick-slip behavior and an increase of pullout force with decreasing embedded length. The results have implications for CNT composite strength and toughness.

DOI: 10.1103/PhysRevB.69.233408 PACS number(s): 62.25.+g, 31.15.Qg, 61.46.+w, 62.20.Qp

Carbon nanotubes (CNTs) are attractive as high-performance nanoscale reinforcements owing to their extremely high stiffness and high strength. Significant enhancements in stiffness, strength, and fracture toughness have been reported for polymers, metals or ceramics composites containing small volume fractions of CNTs.[1–5] An important issue in CNT composites is load transfer between matrix and CNTs, and between walls of multiwall CNTs. Load transfer plays several roles; most important are its effects on composite strength and toughness. Assuming frictional sliding with an interfacial sliding stress τ acting along the entire embedded length of a fracture fiber, the tensile strength and work-of-fracture scale as $\tau^{-1/m}$ and $\tau^{-m-1/m+1}$, respectively, where m is the Weibull modulus describing the statistical distribution of nanotube strengths.[6] Therefore, independent of the reference nanotube strength (e.g., average tensile strength at some specified gauge length), composite strength depends on the strength and nature of the friction, and can approach zero for low τ, while the work of fracture could be large. The precise origins of CNT sliding behavior and the magnitude of the sliding force are thus key to understanding and optimizing CNT/composite behavior.

Here, we consider the sliding behavior of multiwall CNTs with the inner wall(s) broken and being pulled out of the outer walls. This "sword-and-sheath" deformation is of interest in its own right,[7–10] but can also be viewed as a composite system wherein the outer walls represent a matrix material surrounding a broken nanotube. We demonstrate that the "frictional" sliding in fractured CNTs is not frictional in nature because: (i) the force to pull out the inner walls of a multiwall CNT (MWCNT) is independent of the embedded length and (ii) the force is controlled by deformations at the embedded "fractured" end of the inner nanotube walls. Issue (i) also applies to capped-end nanotubes, due to the change in surface energy as smooth graphiticlike walls are pullout. However, for fractured nanotubes, a critical force is required to pull the fractured walls ends through the outer wall (s). Our results are in quantitative agreement with explicit experiments on the direct pullout of inner CNT walls from outer CNT walls. We also show that a uniform applied lateral force (normal pressure) on the outer CNT wall leads to a large increase in the pullout force for fractured tubes, from which a true local friction coefficient can be obtained, and that local regions of pressure or defects in the outer wall lead to large variations in the pullout force as the fractured end of the inner wall slides by the local anomaly. This suggests that statistical defects in the MWCNTs can cause the stick-slip behavior and increasing sliding resistance with decreasing embedded length, as observed experimentally.

Molecular dynamics has been used extensively to study nanotube deformation and pullout. Qian *et al.* have predicted the load transfer between CNT bundles[11] while Frankland and Harik analyzed the pullout force of CNTs from a polymer matrix.[12] Based on molecular dynamics simulations, MWCNTs have been proposed as gigahertz nanooscillators or nanoscale damped springs[10,13] Sliding of multiwall nanotubes has been considered within the context of nanobearings, but nanotube pullout and the influence of pressure and defects have not previously been studied.

Here, the molecular dynamics (MD) method was used to simulate nanotube pullout for a variety of geometries at near-zero temperature. Double-wall MWCNTs in the zigzag and armchair configurations were generated, with the inner wall tube protruding out from the end of the outer wall. The embedded end of the inner wall was either capped, by connecting dangling C bonds appropriately, or fractured (see Fig. 1). Inner nanotube diameters of about $d = 1-5$ nm and typical lengths of $L = 8-10$ nm were used for most of the calculations but other lengths and multiwall nanotubes were also studied. The Tersoff-Brenner potential was used to represent

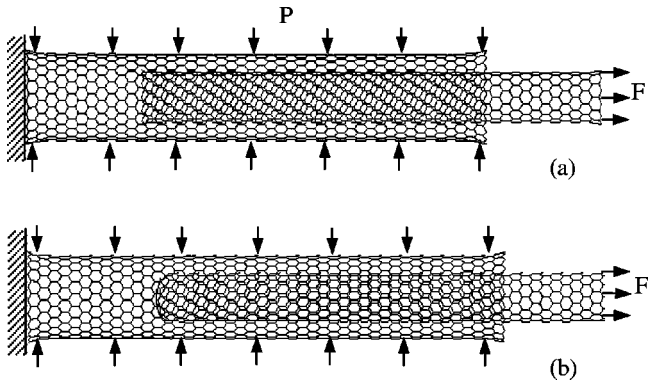

FIG. 1. Multiwall CNT pullout geometries for (a) fractured and (b) capped-end inner nanotube walls. Note outward splaying of the fractured nanotube ends.

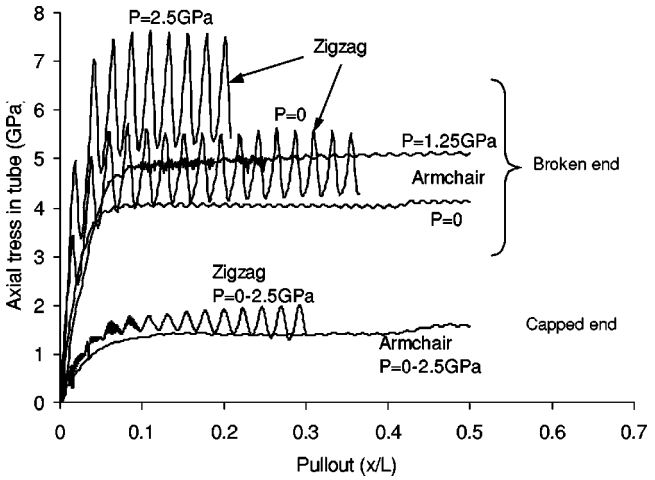

FIG. 2. Pullout stress versus pullout length, for various nanotubes and applied pressures ($L=9.6$ nm, inner wall diameter =1 nm).

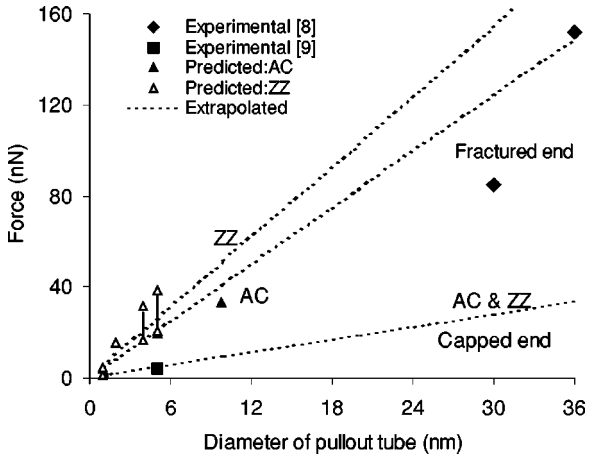

FIG. 3. Pullout force versus nanotube diameter for fractured and capped inner nanotube walls, as obtained by MD (triangles: fractured end; circle: capped end), as extrapolated using a diameter-independent pullout stress (dashed lines), and by experiment (Akita and Nakayama (Ref. 9) solid square; Yu *et al.* (Ref. 8): solid diamond). *ZZ*: zigzag, AC: armchair.

the intrawall C—C bonding.[14] The interwall interaction was modeled by a Lennard-Jones potential $E(r)=4e[(r_0/r)^{12}-(r_0/r)^6]$ with $r_0=3.468$ Å and $e=2.86$ meV, a model used successfully in C_{60} interactions and adequate for our purposes.[15] The range of this potential was taken as 20 nm so that the long-range effects of the van der Waals potential were appropriately included. Note that there is no direct C—C bonding across the nanotube walls in any cases studied here. In the simulation, the inner tube was pulled out in displacement increments of 0.1 Å, with relaxation to equilibrium at a temperature of 0.05 K after each increment, by moving the last four rings at the exposed end of the inner nanotube rigidly as a unit. Similar conditions were imposed on the exposed end of the outer nanotube (Fig. 1). A radial normal pressure p was applied in some cases to assess frictional sliding. For a given applied displacement of the inner nanotube wall, we measure the applied pullout force F and calculate the pullout stress $\sigma=F/A$, where A is the effective cross section of the inner tube, $A=\pi d/t$ with $t=3.44$ Å the nominal interwall spacing.

Figure 2 shows the measured pullout stress as a function of sliding distance for defect-free armchair and zigzag nanotubes. After an initial loading portion, a "sliding" regime ensues as the inner wall is gradually pulled through the outer wall. In the sliding regime, there is no dependence of the pullout stress on the embedded length or the number of walls and, moreover, there is a markedly different magnitude of the pullout force for the different end conditions: The "fractured" end exhibits a pullout force 3–4 times larger than that of the capped end for both types of nanotubes. The average pullout forces associated with the capped end nanotubes are essentially equal to the (slightly diameter-dependent) surface energy, as verified by our independent calculations and as anticipated by previous work.[10,16] The larger forces obtained for the fractured ends are due to the interaction of the splayed fractured end (Fig. 1) as it is dragged through the outer nanotube. This can be seen explicitly by the large peaks in the distribution of stresses along the nanotubes and by the radial displacements of the outer nanotube around the fractured embedded end. Note that the initiation of slip, and associated "friction," is independent of how the excess energy is subsequently dissipated. *Thus, the "sliding" friction behavior in fractured MWCNTs is not frictional at all: It is controlled by a maximum shear strength for sliding of the inner fractured end defect against the outer walls.*

The calculated pullout forces for the various nanotube types and end conditions are shown versus nanotube diameter in Fig. 3. The capped end case shows a linear dependence on diameter (constant stress), as expected. The fractured end case also shows a linear trend with diameter but with some variations: Armchair CNTs increase slower than linearly and zigzag CNTs increase faster. For double-walled CNTs, the splayed end of larger diameter zigzag nanotubes undergoes a buckling behavior, leading to a decreased pullout force once the fractured end enters the outer nanotube; the peak force before steady state force and after buckling are both shown in Fig. 3. For tripled-walled tubes with two inner walls fractured, buckling is suppressed; this buckling will be the subject of future work. Using the linear extrapolation of the small diameter nanotube simulations, i.e., assuming a constant pullout stress, we can compare our (quasistatic) MD results against the experimental data on pullout reported by Akita and Nakayama[9] and Yu *et al.*,[8] obtained at slow pullout rates. In Akita's experiments, $d=5$ nm and the outer layers of MWCNTs were pulled from an end-capped inner walls with a constant force of 4.2 nN. Our calculation for the capped nanotubes, scaled to the experimental diameter, is 5.1 nN (Fig. 3), in agreement with experiment and consistent with previous calculations and measurements for capped end sliding.[7,9,10] The experiments by Yu *et al.* are similar to those by Akita and Nakayama, but the nanotubes are large in diameter and the outermost shells were broken by extension. The data of Yu *et al.* are also shown in Fig. 3 and agree well with the predictions for the *fractured-end* nanotubes. *Our calculations thus quantitatively rationalize the notable differences in pullout forces between the two sets*

of data: One set corresponds to capped ends and the other to fractured ends.

For the fractured-end nanotube case expected to be relevant in composites, the pullout force is controlled by mechanical interlocking of the end defect with the outer walls or surrounding matrix material. In realistic composites, the nanotube/matrix interface may be rough, wavy, or defective. We have thus performed several calculations to demonstrate the effects of such complications on the pullout stress.

Figure 2 shows typical results of the pullout stress under an applied radial pressure p. For the capped nanotubes, there is essentially no pressure effect, indicating nearly zero friction coefficient and consistent with prior work.[7,9,10] For the fractured nanotubes, however, the pullout stress rises linearly with applied pressure. The pressure effect is thus also controlled by the fractured end, and leads to a traditional "sliding friction" over a small region near the end of the tube, $F_{\|}=F_{0\|}+\mu F_{\perp}$. The friction is consistent with Amonton's law $\tau=\tau_0+\mu p$, if the "area of contact" is confined to a width w at the fractured end $[\tau=F_{\|}/(\pi dw), p=F_{\perp}/(\pi dw)]$. By analyzing the deformation of the outer tube due to the splayed inner fractured end, we estimate an effective interaction width $w=4.1$ Å, from which we then deduce a friction coefficient of $\mu=0.13$ for the zigzag nanotube and $\mu=0.33$ for the armchair nanotube. Note that (i) this friction only acts over the width w and not over the entire embedded nanotube length and (ii) Amonton's law is obtained nanoscopically without the intervening absorbed layers needed for obtaining the law macroscopically.[17]

The frictional behavior shown in Fig. 2 demonstrates that the pullout stress will vary due to nonuniform pressure, which we have simulated explicitly, and hence both stick-slip behavior and increasing pullout force with decreasing embedded length, can exist.

Mechanical interlocking of the embedded end with various defects on the outer nanotube can also modify the pullout stress or force, and lead to the length-dependent friction and stick-slip behavior observed by Yu *et al.* This was studied by introducing a circumferential array of Stone-Wales 5/7/7/5 defects into the outer wall,[18] causing the wall to become locally curved: concave for the armchair and convex for the zigzag; again no C—C bond formation between walls is permitted. Figure 4 (curve C) shows the significant pullout stress caused by 3 or 12 Stone-Wales defects interacting with the inner fractured end in an armchair nanotube. Interaction with an inner capped-end shows a significant decrease in the pullout stress, an effect not driven simply by surface energy. For zigzag nanotubes, the pullout stress decreases rapidly as the inner fractured end encounters the dislocations, due to relief of the radial constraint. It is possible that such defects could be dragged along with the end during pullout, leading to rate and temperature-dependent forces, but this phenomenon has not been investigated here since we do not permit C—C bond breaking and reforming. The pullout stress can also be influenced by the interaction between defects on the inner and outer walls, in the absence of any interaction with the embedded end. Figure 4 (curve A) shows the pullout stress due to interactions between three Stone-Wales defects on the outer wall and three vacancies on the inner wall of an armchair CNT: When the vacancies slide

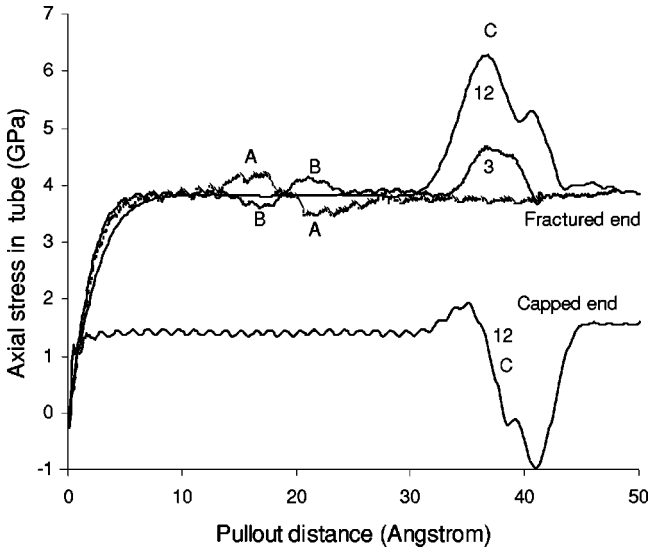

FIG. 4. Pullout stress versus distance for a fractured defective inner wall nanotube sliding within a defective outer wall nanotube, for several types of defects on the outer wall (armchair). Pullout stress varies as the fractured end (curve C), three vacancies (Curve A), and three Stone-Wales defects (curve B), meet three Stone-Wales defects in the outer wall, respectively.

past the dislocations, the pullout stress increases. When the voids are replaced by Stone-Wales defects, the pullout force first drops but then increases (Fig. 4, curve B). In all cases, there is an increase in the pullout stress at some point during the pullout, which sets the stage for stick-slip behavior under either constant force loading, or constant displacement loading with large embedded lengths that store elastic energy.

The implications of these results for composite performance are interesting. First, for the idealized composite consisting of aligned nondefective nanotubes, the absence of a traditional "frictional" sliding along the entire nanotube length implies that there is no finite *in situ* gauge length at which nanotube strength can be measured;[6] the relevant length is the longitudinal sample size and so the characteristic nanotube strength tends toward zero as the sample size increases. This situation is avoided if frictional sliding can occur. However, lateral applied pressure does not lead to standard frictional behavior, but rather only to frictional behavior near the end of the CNT. Our results suggest that heterogeneity in the form of distributed defects and distributed lateral pressures acting on each of the CNTs in a collection of aligned CNTs could lead to an effective frictionlike behavior. Such a transition to macroscale friction remains to be investigated. The enhanced load-carrying capability of the fractured nanotubes as found here can be helpful for composite strength and toughness. For a CNT area fraction f (including the interior pore space), the minimum ultimate strength is set by the pullout stress as $\sigma_{\min}^{\text{uts}}=f(4t/r)\ \sigma_{\text{pullout}}$, which can be ~ 1 GPa. The composite toughness is the work per unit area required to pull the embedded CNTs out of the matrix or surrounding walls, and is thus $W=f(4t/r)\ \sigma_{\text{pullout}}L$, where L is the embedded length after nanotube fracture.

In summary, MD simulations of pullout of fractured inner walls from the outer walls of a multiwall nanotube shows

that the pullout force is dominated by end effects. Our results explain varying experimental data on the pullout forces, both qualitatively and quantitatively. Local pressure can generate local frictional sliding, and distributed pressure or defects in the nanotube walls can increase and decrease the pullout force, depending on the defect geometry, permitting stick-slip behavior as observed experimentally. This initial work has a variety of implications for composite behavior that can only be resolved by future work on the connections between macroscale versus nanoscale friction, for which nanotubes may represent a unique laboratory.

Z.X. and W.A.C. thank Professor K. S. Kim (Brown), Professor Y. W. Zhang (National University of Singapore), and Professor R. Ruoff (Northwestern) for helpful discussions.

[1] P. M. Ajayan, L. S. Schadler, C. Giannaris, and A. Rubio, Adv. Mater. (Weinheim, Ger.) **12**, 750 (2000).
[2] D. Qian E. C. Dickey, R. Abdrews, and T. Rantell, Appl. Phys. Lett. **76**, 2868 (2000).
[3] G.-D. Zhan, J. Kuntz, J. Wan, and A. K. Mukherjee, Nat. Mater. **2**, 38 (2003).
[4] M. J. Biercuk, M. C. Llaguno, M. Radosavljevic, J. K. Hyun, A. T. Johnson, and J. E. Fischer, Appl. Phys. Lett. **80**, 2767 (2002).
[5] M. Choi, R. Yong, and R. Yoo, Nat. Mater. **2**, 473 (2003).
[6] W. A. Curtin, Adv. Appl. Mech. **36**, 164 (1999).
[7] J. Cumings and A. Zettl, Science **289**, 602 (2000).
[8] M. F. Yu, B. I. Yakobson, and R. S. Ruoff, J. Phys. Chem. **104**, 8764 (2000).
[9] S. Akita and Y. Nakayama, Jpn. J. Appl. Phys., Part 1 **42**, 3933 (2003).
[10] S. B. Legoas, V. R. Coluci, S. F. Braga, P. Z. Coura, S. O. Dantas, and D. S. Galvao, Phys. Rev. Lett. **90**, 055504 (2003).
[11] D. Qian, W. K. Liu, and R. S. Ruoff, Compos. Sci. Technol. **63**, 1561 (2003).
[12] S. J. V. Frankland and V. M. Harik, Surf. Sci. **525**, L103 (2003).
[13] J. L. Rivera, C. McCabe, and P. T. Cummings, Nano Lett. **3**, 1001 (2003).
[14] D. W. Brenner, Phys. Rev. B **42**, 9458 (1990).
[15] L. A. Girifalco, M. Hodak, and R. Lee, Phys. Rev. B **62**, 13 104 (2000).
[16] A. N. Kolmogorov and V. H. Crespi, Phys. Rev. Lett. **85**, 4727 (2000).
[17] A. R. C. Baljon and M. O. Robbins, Science **271**, 482 (1996).
[18] J. Stone and D. J. Wales, Chem. Phys. Lett. **128**, 501 (1986).